



ORIGINAL ARTICLE

Clinical exome sequencing identifies novel *CREBBP* variants in 18 Chinese Rubinstein–Taybi Syndrome kids with high frequency of polydactyly

Sha Yu¹  | Bingbing Wu^{1,2} | Yanyan Qian^{1,2} | Ping Zhang^{1,2}  | Yulan Lu^{1,2} | Xinran Dong^{1,2} | Qing Wang¹ | Xuemei Zhao^{1,2} | Renchao Liu^{1,2} | Wenhao Zhou^{1,2,3} | Huijun Wang^{1,2} 

¹Key Laboratory of Birth Defects, Pediatrics Research Institute, Children's Hospital of Fudan University, Shanghai, China

²Center for Molecular Medicine, Pediatrics Research Institute, Children's Hospital of Fudan University, Shanghai, China

³Departments of Neonatology, Children's Hospital of Fudan University, Shanghai, China

Correspondence

Wenhao Zhou, Departments of Neonatology, Children's Hospital of Fudan University, 399 Wanyuan Road, Shanghai 201102, China.
Email: zhouwenhao@fudan.edu.cn

Huijun Wang, Pediatrics Research Institute, Children's Hospital of Fudan University, 399 Wanyuan Road, Shanghai 201102, China.
Email: huijunwang@fudan.edu.cn

Funding information

Shanghai Key Laboratory of Birth Defects, Grant/Award Number: 13DZ2260600; National Key Research and Development Program, Grant/Award Number: 2018YFC0116903; National Natural Science Foundation of China, Grant/Award Number: 81741036

Abstract

Background: Rubinstein–Taybi syndrome (RSTS) is a rare genetic disease characterized by broad thumbs and halluces, facial dysmorphisms, short stature, and intellectual disability. RSTS is mainly caused by de novo variants in epigenetics-associated gene, *CREBBP*. To date, there is no cohort study of *CREBBP* variants in Chinese RSTS patients.

Methods: In this study, 18 kids who meet the main criteria of RSTS were recruited. Molecular diagnoses were analyzed by clinical exome sequencing (CES), and the medical records were reviewed retrospectively.

Results: Nineteen novel *CREBBP* variants in 18 RSTS patients were identified, including two missense, four nonsense, five frameshift, one splicing variants, and seven intragenic deletions. A higher incidence (37%, 7/19) of intragenic deletions was detected. One patient who had two de novo missense variants c.[4112T > A, 4118C > A] in cis and one patient who had a de novo frameshift variant c.5837delC in homozygous state (90%) were found in this study. Compared with the previously reported populations, seven clinical features were different, including the higher incidence of polydactyly, syndactyly, microcephaly, and micrognathia, and the lower incidence of angulated thumbs, autistic behavior, and epilepsy. One patient with obesity in the first year was diagnosed with *CREBBP* gene exon 2 deletion, was initially suspected of Prader–Willi syndrome.

Conclusion: We reported the genetic and clinical information of 18 RSTS patients from Chinese population with novel *CREBBP* variants. This study provides a new insight into RSTS and illustrates the value of applying CES which increases the diagnostic yields and enhances the clinical care of RSTS patients.

KEYWORDS

clinical exome sequencing, *CREBBP*, polydactyly, Rubinstein–Taybi syndrome

Sha Yu and Bingbing Wu contributed equally to this work.

This is an open access article under the terms of the Creative Commons Attribution-NonCommercial-NoDerivs License, which permits use and distribution in any medium, provided the original work is properly cited, the use is non-commercial and no modifications or adaptations are made.

© 2019 The Authors. *Molecular Genetics & Genomic Medicine* published by Wiley Periodicals, Inc.

1 | INTRODUCTION

Rubinstein–Taybi syndrome (RSTS; OMIM 180849) is a rare multiple congenital abnormality syndrome, with an estimated incidence of 1:125,000 live births (Hennekam, 2006). This condition was first described in 1963 by Dr. Jack Rubinstein and Dr. Hooting Taybi (Rubinstein & Taybi, 1963). The main manifestations of the disease include distinctive facial features, broad thumbs and big toes, postnatal growth delay, and mild to severe intellectual disability (Milani et al., 2015; Rubinstein & Taybi, 1963).

RSTS is an autosomal dominant inherited disorder mainly caused by variants in the homologous genes *CREBBP* (OMIM 600140) and *EP300* (OMIM 600140); however, most cases of RSTS are sporadic. Several studies revealed about 55% and 8% of RSTS patients are caused by mutant *CREBBP* and *EP300* genes, respectively, while the cause of the rest case is not defined (Rusconi et al., 2015). The rare heterozygous variants found in *CREBBP* typically arise de novo although several RSTS cases were inherited (Bartsch et al., 2010; Negri et al., 2015). The mutational spectrum of *CREBBP* consists of point variants (30%–50%) and deletions (~10%; Rusconi et al., 2015). CBP (also known as cAMP response element-binding protein (CREB)-binding protein, encoded by *CREBBP* gene) is a coactivator for numerous transcription factors that can influence diverse physiological processes (Shiama, 1997). CBP is ubiquitously expressed and was demonstrated to possess an intrinsic histone acetyltransferase (HAT) activity which influences chromatin activity via modulating nucleosomes histones (Chan & Thangue, 2001). Moreover, previous research demonstrated that point variants affected mainly the HAT domain of CBP that the loss of HAT activity is sufficient to cause RSTS (Kalkhoven et al., 2003).

Despite the hallmarks of RSTS, striking facial feature, broad thumbs and hallux, the diagnosis of RSTS is sometimes challenging because of the high variability in phenotype and genotype (Spena, Gervasini, & Milani, 2015). Clinical exome sequencing (CES) is a reliable and rapid diagnostic tool for suspected genetic disorders, and has been powerfully used in medical practices (Lee et al., 2014). What is more, with the rapid development of the bioinformatics algorithm, copy number variations (CNV) can be detected coupled with point variants and indels simultaneously. Implementation of this strategy can increase diagnostic yields and enhance clinical care (Ellingford et al., 2017).

To our knowledge, no cohort study of *CREBBP* variants in Chinese RSTS patients has been reported currently. Here, we analyze the clinical and genetic characterization of 18 RSTS patients who had pathogenic variants in *CREBBP* gene detected by CES. More importantly, the clinical characteristics of patients with *CREBBP* variants in China were compared with those patients reported in western countries. This

research can provide some new insight for the genotype and phenotype of RSTS.

2 | MATERIALS AND METHODS

2.1 | Patients

From May 2014 to July 2018, patients referred to our laboratory for genetic test and fulfilled the following criteria were analyzed for *CREBBP* variants: (a) less than 17 years of age, (b) clinical information was available, and (c) strong suspected genetic disorders. Clinical manifestations, biochemical tests, and imagological exam results were obtained from both electronic medical records and patients' parents. Birth weight, occipitofrontal circumference (OFC), height, and weight were evaluated based on the clinical used criteria from Chinese reports (Li, 2009; Zhu et al., 2015).

The genetic testing was approved by the ethics committees of Children's Hospital, Fudan University (2014-107 and 2015-130). Informed consents were obtained from patients' parents.

2.2 | Genetic studies

2.2.1 | Variant analysis using Clinical exome sequencing

Genomic DNA was extracted from whole blood using the QIAamp DNA Blood Mini Kit (QIAGEN, Germany) according to the manufacturer's protocol. DNA fragments were enriched for panel sequencing using the Agilent ClearSeq Inherited Disease panel kit (2,742 genes; #3, #4, #5, #7, #8, #9, #10, #12, #13, #14, #15, #16, #17, #18) or exome sequences using the Agilent SureSelect XT Human All Exon 50 Mb kit (#1, #2, #6, #11). *CREBBP* variants were identified from the Clinical exome sequencing (CES) data.

Sequence data were mapped to the human reference genome (GRCh37/hg19). Variants were annotated by ANNOVAR and VEP software (McLaren et al., 2010), with a minor allele frequency of less than 5% according to either the 1,000 Genomes Project or the Exome Aggregation Consortium (ExAC). We used the CANOES tool to detect CNV from exon-based reads count (Backenroth et al., 2014). Detected CNVs were further annotated and filtered, considering the known pathogenicity, variant size, and affected genes of CNV. Detail workflow of CNV screening was described in our previous study (Qian et al., 2018). Missense variants were evaluated by the SIFT, PolyPhen2.2, and MutationTaster (Adzhubei et al., 2010; Kumar, Henikoff, & Ng, 2009; Schwarz, Rödelsperger, Schuelke, & Seelow, 2010). The effect of variants on splicing was predicted by Human Splicing Finder v.3.1 (HSF; <http://www.umd.be/HSF3/HSF>; Desmet et al., 2009).

The pathogenicity of the candidate variants was analyzed according to the standards and guidelines recommended by the American College of Medical Genetics and Genomics (ACMG; Richards et al., 2015) and only pathogenic variants were enrolled in the present study. The candidate variants were validated by Sanger sequencing on an ABI 3730 Genetic Analyzer (Applied Biosystems), and the same variant was detected in their parents to confirm whether the variant was germline derived.

2.2.2 | Prediction of protein structure

The 3D models of human wild-type *CREBBP* and its mutant proteins (V1371D, P1373H) were performed using Mutalyzer (<https://www.mutalyzer.nl/>) and Swiss-model servers (<https://www.swissmodel.expasy.org>). We selected template 5 μ 7g.1A as the protein structure template (Park et al., 2017) and used computer program MODELLER (Martí-Renom et al., 2000) for automated modeling. The protein structures were visualized with PyMOL 1.7.4.5. To predict the secondary structure of wild-type *CREBBP* and its mutant proteins (V1371D, P1373H), we used an online software platforms SOPMA (https://npsa-prabi.ibcp.fr/cgi-bin/npsa_automat.pl?page=npsa_sopma.html).

2.2.3 | Real-Time quantitative PCR

Seven pathogenic small deletions in 16p13.3 identified by exome sequencing were confirmed by quantitative PCR (qPCR) assay. The assay was performed using TaKaRa SYBR[®] Premix Ex Taq[™] II kit (Tli RNaseH Plus) on the ABI StepOnePlus[™] Real-Time PCR System (v.2.0). Three to five primer pairs for each CNV were designed. The real-time PCR mixture (10 μ l) contained 5 μ l SYBR Green MIX, 0.2 μ l ROX dye 50 \times , 0.5 μ mol/L of each primer for the target region and for LDHA as the reference gene, and 20 μ g of DNA. The thermal profile for the qPCR included: a preincubation step of 45 s at 95°C, followed by 40 cycles of amplification (5 s at 95°C, 30 s at 60°C, 30 s at 72°C). The relative quantification analysis was performed with $2^{-\Delta\Delta CT}$ method and one sample *t* test for significance analysis (Schmittgen & Livak, 2008).

2.2.4 | Multiplex ligation-dependent probe amplification

Multiplex ligation-dependent probe amplification (MLPA) experiments were also carried out on the seven 16p13.3 microdeletions. The assay was performed using commercially available SALSA MLPA kits (P313-B2 *CREBBP*, MRC-Holland) following the manufacturer's protocol (Schouten, 2002). The amplification products were separated by capillary electrophoresis using ABI 3130xl genetic analyzer (Applied Biosystems). Data were visually inspected and

analyzed using GeneMarker software V2.7.0 (SoftGenetics, LLC). All samples were found with dose imbalances were tested at least twice.

3 | RESULTS

3.1 | Clinical characteristics

Investigation of patients using CES and complementary technologies showed 19 pathogenic variations of *CREBBP* gene in 18 unrelated patients, who met the main criteria of RSTS described in literatures. Seventeen patients were of Chinese Han, one was of Uyгур (#12). The average diagnosis age was 17 months (from 2 months to 12 years), while four patients died in neonate (#14, #16, #17, #18) and one died at 4 months (#1). Detailed clinical findings are summarized in Table 1. The photographs of face and limb are illustrated in Figure 1.

3.1.1 | Facial dysmorphisms

All these patients have typical facies, including micrognathia (18/18), heavy/ arched eyebrows (16/16), down-slanted palpebral fissures (16/16), low set ears (16/16), hypertelorism (16/16), arched palate (16/16), grimacing smile (13/13), et al. The relatively prominent beaked nose was observed in 15/16 of patients (#14 and #17 photographs not available). Moreover, eyelid ptosis was observed in 57% of patients (8/14) and all were in left-eyelid ptosis.

3.1.2 | Organ malformations

All of these 18 patients showed broad big toes and widen distal phalanges, 16 of them had broad thumbs, which were the most common anomalies of skeleton in reported literatures. In addition, polydactyly (2/18), syndactyly (2/18), polysyndactyly (3/18), and congenital hip dysplasia (2/16) were observed, which were rarely reported. However, angulate thumbs (2/18) and angulate big toe (3/18) were relatively rare in our patients.

Brain MRI records were available for 14 patients, 57% (8/14) of them exhibited brain structural abnormalities. Abnormality of the corpus callosum was reported in 29% (4/14) of patients (#6, #7, #13, #15); delayed myelination was reported in 21% (3/14) of patients (#3, #9, #15); abnormality of lateral ventricle was observed in 19% (3/14) of patients (#2, #6, #7); and Chiari malformation type 1 was observed in patient #6 (Figure 4).

Ocular anomalies were reported in 38% of patients (6/16), including extra- and intra-ocular abnormality. Patient #7 had strabismus, corneal leukoma, glaucoma, nystagmus, iris abnormalities simultaneously, with TORCH test positive. Other four patients (#2, #6, #8, #9) presented with strabismus, patients #1 with corneal leukoma, patient #2 with mild hypermetropia. Patients #6 and #7 presented with bilateral congenital

TABLE 1 Summary of clinical features in 18 individuals with *CREBBP* mutations

Patient	#1	#2	#3	#4	#5	#6	#7	#8	#9	#10
Genotype	c.1941+1G>T	c.[4112T>A, 4118C>A]p.V1371D; p. P1373H	c.3459C>G	c.4660A>T	c.5638C>T	c.5905C>T	c.1062dupA	c.1129_1131delinsCAATG, p. V377Qfs*13	c.1279_1280delTTG	c.2459delC
Zygoty	Het	Het	Het	Het	Het	Het	Het	Het	Het	Het
Inheritance	De novo	De novo	De novo	De novo	De novo	De novo	De novo	De novo	De novo	De novo
Gender	F	F	M	M	F	M	F	M	F	F
Main complaint	Pneumonia	Feeding problems	Pneumonia	Jaundice	Feeding problems	Pneumonia	Pneumonia	Pneumonia	DD	DD
Age at onset	28 days	5 days	2 months	3 days	3 days	3 days	26 days	6 months	9 months	1 months
Age at diagnosis (months)	4 months	5 months	4 months	5 months	4 months	3 months	2 months	8 months	18 months	2 months
Current age (months)	Died (4) ^a	20 months	8 months	20 months	5 months	48 months	21 months	13 months	45 months	2 months
Patient stayed in NICU	+	-	+	-	-	+	+	+	-	+
Age of father/mother (years)	24/23	33/31	26/33	22/25	28/28	30/29	27/29	31/31	34/31	36/35
Prenatal period										
TORCH tests	-	-	-	-	-	-	+	-	-	-
Polyhydramnios	-	+	+	+	-	+	+	-	-	-
Intrauterine growth restriction	-	+	-	-	+	-	-	-	-	+
Birth weight (g) ¹	3,100 (10–25th)	3,250 (50–75th)	3,320 (50–75th)	2,500 (<3rd)	2,000 (<3rd)	2,300 (<3rd)	3,130 (25–50th)	3,340 (50–75th)	3,700 (90–97th)	1,820 (<3rd)
Gestational age (weeks)	41	37	38	38	37	38	39	38	38	36
Postnatal growth										
Feeding difficulties	+	+	+	-	+	+	+	+	-	+
Height ²	<-3 SD	<-2 SD	<-3 SD	<-3 SD	<-3 SD	<-2 SD	<-2 SD	<-1 SD	<-2 SD	<-3 SD
Weight ³	<-1 SD	<1 SD	<-3 SD	<-2 SD	<-3 SD	<-2 SD	<-1 SD	<-2 SD	<-3 SD	<-2 SD
OFC ⁴	<-2 SD	<-3 SD	<-3 SD	<-3 SD	<-3 SD	<-3 SD	<-1 SD	<-2 SD	<-2 SD	<-2 SD
Psychomotor development										
Crawled	-	20 m	-	18 m	-	20 m	21 m	-	23 m	-
Sat up	-	16 m	-	8 m	-	10 m	20 m	13 m	18 m	-
Walked	-	-	-	-	-	39 m	-	-	34 m	-

(Continues)

TABLE 1 (Continued)

Patient	#1	#2	#3	#4	#5	#6	#7	#8	#9	#10
First words	-	-	-	14 m	-	>48 m	-	-	35 m	-
3-word phrases	-	-	-	-	-	>48 m	-	-	>45 m	-
Toilet trained	-	-	-	-	-	-	-	-	-	-
Behavioral problems	-	+	-	-	-	+	+	-	-	-
Facial dysmorphism										
Microcephaly (<-2 SD)	+	+	+	+	+	+	-	+	+	+
Eyelid ptosis	+	-	-	-	+	+	+	+	+	-
Down-slanted palpebral fissures	+	+	+	+	+	+	+	+	+	+
Heavy/ arched eyebrows	+/+	+/+	+/+	+/+	-/+	-/+	+/+	+/+	+/-	+/+
Hypertelorism	+	+	+	+	+	+	+	+	+	+
Low set ears	+	+	+	+	+	+	+	+	+	+
Prominent beaked nose	+	+	-	+	+	+	+	+	+	+
Grimacing smile	+	+	+	+	+	+	+	+	+	+
Micrognathia	+	+	+	+	+	+	+	+	+	+
Hands and Feet										
Broad/angulated thumb	+/-	+/-	+/-	+/+	-/-	+/-	+/-	+/-	+/-	+/-
Broad/angulated hallux	+/-	+/+	+/-	+/-	+/+	+/-	+/+	+/-	+/-	+/-
Syndactyly/polydactyly	+/+	-/-	-/-	+/+	-/+	+/+	-/-	-/-	-/-	-/+
Widened distal phalanges	+	+	+	+	+	+	+	+	+	+
Major malformations										
Brain MRI abnormalities	NA	ALV	Delayed myelination	-	-	ACC; Chiari malformation; ALV	ACC; ALV	-	Delayed myelination	Neonatal encephalopathy
Ocular anomalies	Corneal leucoma	Strabismus	-	-	-	NLDO, strabismus	NLDO, Corneal leucoma/Glaucoma/nystagmus/strabismus	Strabismus	Strabismus	-
laryngeal cartilage anomalies	+	+	+	+	+	+	+	+	-	+
Cardiovascular anomalies	PDA, ASD, PH	PFO	PFO	PDA, ASD, PFO	PFO	PDA, PFO, PH, ASA	PDA, PFO	-	-	-

(Continues)

TABLE 1 (Continued)

Patient	#1	#2	#3	#4	#5	#6	#7	#8	#9	#10
Genital anomalies	-	-	+	+	-	-	-	+	-	-
Anomalies of hip joint	-	+	-	-	-	+	-	-	-	-
Medical complications										
Neonatal hyperbilirubinemia	-	+	+	+	+	+	+	-	-	-
Respiratory infection/age ⁵	+	-	+	+18 m	+	+36 m	+>21 m	+7 m	-	+
Gastroesophageal reflux	+	+	+	-	+	+	+	-	-	+
Constipation/age ⁵	-	+>20 m	-	+15 m	-	+46 m	+	+	+	+>45 m
Patient	#11	#12	#13	#14	#15	#16	#17	#18	#18	Total (n = 18); Average (Range)
Genotype	c.5837delC	Deletion (ex 2)	Deletion (ex 2)	Deletion (ex 1-2)	Deletion (ex 12-31)	Deletion (ex 13-16)	Deletion (ex 21-28)	Deletion	Deletion	
	p. Pro1946Hisfs*30	(ex 2)	(ex 2)	(ex 1-2)	(ex 12-31)	(ex 13-16)	(ex 21-28)	(ex 22-23)	(ex 22-23)	
Zygoty	Hom	Het	Het	Het	Het	Het	Het	Het	Het	
Inheritance	De novo	De novo	De novo	De novo	De novo	De novo	De novo	De novo	De novo	
Gender	F	F	F	F	M	M	M	M	M	10 F/8 M
Main complaint	Syndactyly	Obesity	Pneumonia	Septicemia	DD	Feeding problems	Pneumonia	Pneumonia	Pneumonia	7/18 Pneumonia, 4/18 DD
Age at onset	1 months	7 months	5 months	3 days	40 months	3 days	1 day	6 days	123 days (1 day-40 months)	
Age at diagnosis (months)	4 months	12 years	12 months	18 months	47 months	6 months	18 months	2 months	17 months (2 months-12 years)	
Current age (months)	8 months	12 years	31 months	Death (<1) ^a	51 months	Death (<1) ^a	Death (<1) ^a	Death (<1) ^a	32 months (2 months-12 years)	
Patient stayed in NICU	-	+	-	+	-	+	+	+	11/18	
Age of father/mother (years)	40/37	32/31	28/27	NA	30/27	32/33	NA	29/29	30/30 (22-40/23-37)	
Prenatal period										
TORCH tests	-	-	-	-	-	-	-	-	1/18	
Polyhydramnios	-	-	-	NA	-	-	NA	-	5/16	
Intrauterine growth restriction	-	-	-	NA	-	-	NA	-	3/16	
Birth weight (g) ¹	2,700 (25-50th)	3,450 (90-97th)	2,980 (50-75th)	3,000 (50-75th)	3,500 (50-75th)	2,550 (<3rd)	3,200 (25-50th)	3,300 (25-50th)	5/18 < 3rd	
Gestational age (weeks)	37	36	37	37	38	39	38	40	2/17 < 37	

(Continues)

TABLE 1 (Continued)

Patient	#11	#12	#13	#14	#15	#16	#17	#18	Total (n = 18); Average (Range)
Postnatal growth									
Feeding difficulties	-	+	+	NA	-	+	+	+	13/17
Height ²	<-1 SD	<-2 SD	<-1 SD	NA	<-2 SD	<-3 SD	NA	<-2 SD	6/16 <-3 SD, 1/16 <<-3 SD
Weight ³	<-1 SD	>>3 SD	<-1 SD	NA	<1 SD	<<-3 SD	NA	NA	2/15 <-3 SD, 2/15 <<-3 SD
						SD			
OFc ⁴	<-3 SD	<-2 SD	<<-3 SD	NA	<-1 SD	<-3 SD	NA	<-3 SD	7/16 <-3 SD, 2/16 <<-3 SD
Psychomotor development									
Crawled	-	6 m	18 m	-	20 m	-	-	-	19 m (6-23 m)
Sat up	8 m	6 m	14 m	-	10 m	-	-	-	12 m (6-20 m)
Walked	-	17 m	20 m	-	30 m	-	-	-	28 m (17-39 m)
First words	-	20 m	28 m	-	30 m	-	-	-	25 m (14-35 m)
3-word phrases	-	25 m	>31 m	-	>51 m	-	-	-	25 m
Toilet trained	-	72 m	-	-	-	-	-	-	72 m
Behavioral problems	-	+	-	NA	+	NA	NA	NA	5/14
Facial dysmorphism									
Microcephaly (<-2 SD)	+	+	+	NA	-	+	NA	+	14/16
Eyelid ptosis	+	-	NA	NA	+	-	NA	NA	8/14
Down-slanted palpebral fissures	+	+	+	NA	+	+	NA	+	16/16
Heavy/ arched eyebrows	+/+	+/+	+/+	NA	+/+	+/+	NA	+/+	10/16 +/+, 2/16 +/-, 2/16 +/-
Hypertelorism	+	+	+	+	+	+	+	+	18/18
Low set ears	+	+	+	NA	+	+	NA	+	16/16
Prominent beaked nose	+	+	+	NA	+	+	NA	+	15/16
Grimacing smile	+	+	+	NA	+	+	NA	NA	13/13
Micrognathia	+	+	+	+	+	+	+	+	18/18
Hands and Feet									
Broad/angulated thumb	+/+	+/+	+/+	+/+	-/-	+/+	+/+	+/+	2/18 +/+, 14/18 +/-
Broad/angulated hallux	+/+	+/+	+/+	+/+	+/+	+/+	+/+	+/+	15/18 +/+, 3/18 +/+
Syndactyl/polydactyly	+/+	-/-	-/-	-/-	-/-	-/-	-/-	+/+	3/18 +/+, 2/18 +/-, 2/18 +/-
Widened distal phalanges	+	+	+	+	+	+	+	+	18/18
Major malformations									

(Continues)

TABLE 1 (Continued)

Patient	#11	#12	#13	#14	#15	#16	#17	#18	Total (n = 18); Average (Range)
Brain MRI abnormalities	-	-	ACC	NA	ACC; Delayed myelina- tion	-	NA	NA	8/14
Ocular anomalies	-	-	-	NA	-	-	NA	-	6/16
laryngeal cartilage anomalies	-	-	+	NA	-	+	+	+	13/17
Cardiovascular anomalies	-	-	-	NA	-	ASD	PDA (2mm), PH	ASD, PDA	10/17
Genital anomalies	-	-	-	NA	-	+	NA	+	5/16
Anomalies of hip joint	-	-	-	NA	-	-	NA	-	2/16
Medical complications									
Neonatal hyperbilirubinemia	-	-	-	NA	-	-	NA	-	6/16
Respiratory infection/ age ⁵	-	-	+ / >31 m	NA	-	+	+	+	12/17, 21 m (7–36 m)
Gastroesophageal reflux	-	-	+	NA	-	+	NA	+	10/16
Constipation/age ⁵	-	+ / >12 y	+ / >31 m	NA	-	-	NA	-	9/16, 28 m (12–46 m)

Abbreviations: ACC, abnormality of the corpus callosum; ALV, abnormality of lateral ventricle; ASA, aberrant subclavian artery; ASD, atrial septal defect; DD, developmental retardation; MRI, magnetic resonance imaging; NA, parameter was not assessed; NICU, neonatal intensive care unit; NLDO, nasolacrimal duct obstruction; OFC, occipitofrontal circumference; PDA, patent ductus arteriosus; PFO, patent foramen ovale; PH, pulmonary hypertension; TORCH test: Toxoplasma, Other viruses, Rubella, Cytomegalovirus, and Herpes simplex virus examination

^aAge at death; th, Percentile.

^{1,2,3,4}Parameter was evaluated based on the Chinese reports (Li, 2009; Zhu et al., 2015);

⁵Age to symptom mitigation.



FIGURE 1 Photographs of patient face, hands, and feet described with *CREBBP* variants. Representative facial photograph of patient #6. Micrognathia, arched eyebrows, down-slanted palpebral fissures, hypertelorism, prominent beaked nose, and grimacing smile are observed. Skeletal photographs of the 14 patients. All had broad thumbs/halluces and widened distal phalanges; patients #1, #4, #5, #6, #11 had polydactyly/syndactyly; patients #4 and #11 had angulated thumbs; patients #2 and #8 had angulated hallux

nasolacrimal duct obstruction (CNLDO), and patient #9 had severe bilateral trichiasis and underwent surgery at 3 years old.

Cardiovascular malformations were present in 59% of patients (10/17), from mild patent foramen ovale (PFO), patent ductus arteriosus (PDA), to atrial septal defect (ASD), and aberrant subclavian artery (ASA). Laryngeal cartilage malformation was reported in 76% (13/17) of patients. Urogenital malformation was noted in five patients, including testicular hydrocele (#16) and cryptorchidism (#3, #4, #8, #18). However, none of the patients was noted with abnormality of the kidney.

3.1.3 | Development

Polyhydramnios was observed in 5 of 16 patients (#2, #3, #4, #6, #7), and intrauterine growth restriction (below average) was observed in 19% probands (3/16; #2, #5, #10). Feeding

problems (during neonatal period) were observed in 76% of patients (13/17), and two patients (#5, #7) have been suffering from this problem till now.

During childhood, postnatal growth retardation (weight and/or height < -2 SD) was observed in 89% (16/18) of patients, including one patient (#5) with height $<< -3$ SD and two patients (#5, #16) with weight $<< -3$ SD; while patient #12 presented with obesity from 7 months old. Microcephaly (OFC < -2 SD) was observed in 88% of patients (14/16), and OFC was $<< -3$ SD in two patients (#5, #13; Table S1).

Psychomotor development was evaluated in 13 patients at the follow-up, all of them presented with developmental delay, ranged from mild (#12) to moderate (#2, #4, #7, #8, #13) and severe (#6, #9, #15), three patients (#3, #5, #10, #11) were too young to evaluate the rate. In addition, age of the onset walk was available for five patients and mean

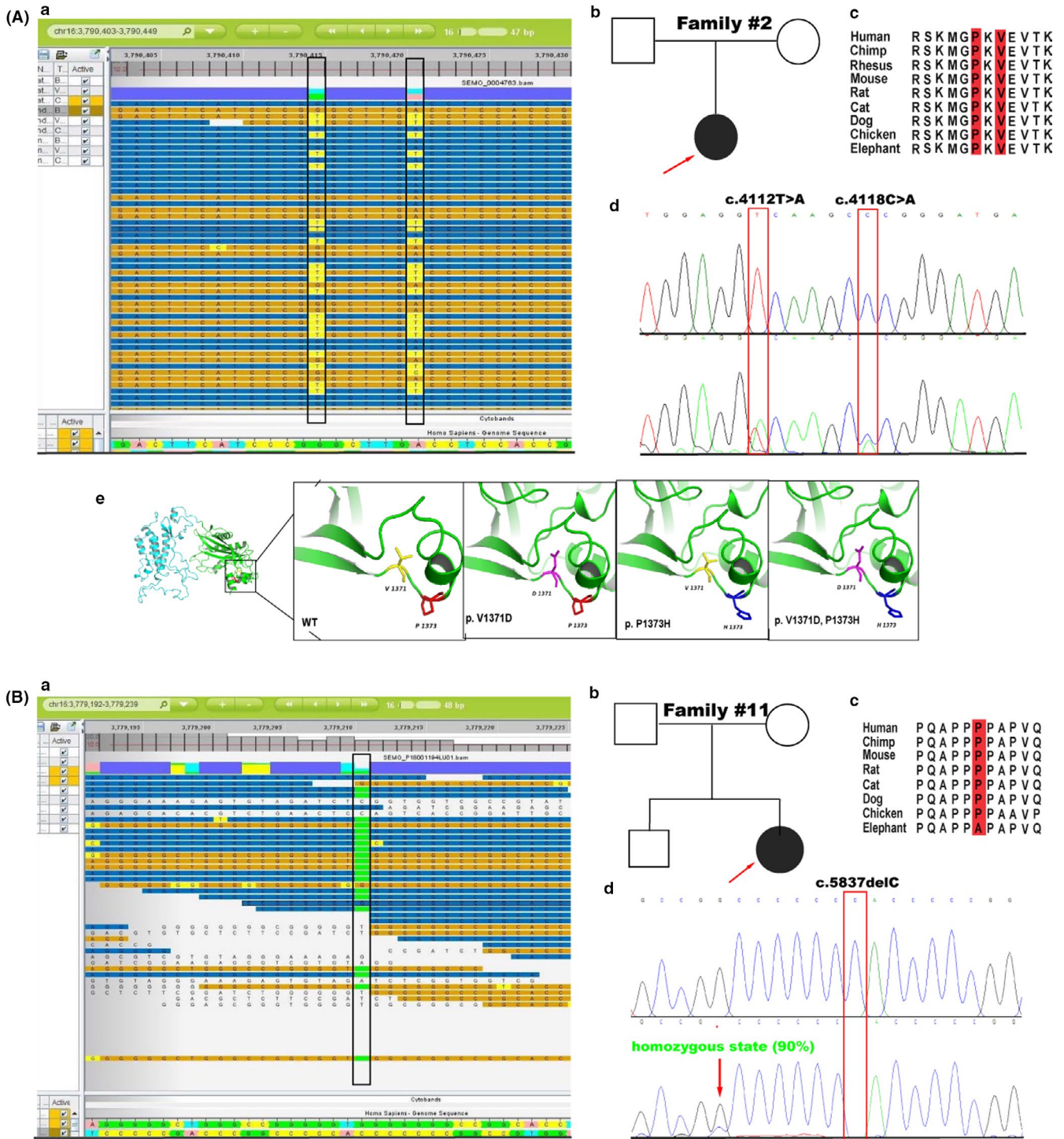


FIGURE 2 Schematic of *CREBBP* with two de novo mutations in patient #2 (a) and homozygous state (90%) de novo mutation in patient #11 (b). a. The sequence reads of the mutation were highlighted in black frames, from Sequence Miner in WuXi NextCODE Genome Browser. b. Pedigree and genotypes of *CREBBP* variations analyzed by Sanger sequencing showing de novo variants. c. Alignment of *CREBBP* orthologues. Amino acids in the mutation site are conserved from human to mouse and are highlight in red frames. d. Sanger sequencing, the presence of the mutated alleles is indicated by red frames e. 3D modeling of *CBP*^{WT} and the *CBP*^{V1371D}, *CBP*^{P1373H}, *CBP*^{V1371D + P1373H} mutants. HAT domain of *CBP* protein is shown as green. The important residues for the changed amino acids are shown as sticks and all of the residues located in the flexure of a loop

age was 28 months; age of the first words was recorded for five patients and mean age was 25 months, and one patient (#6) did not speak at 4 years old. Behavioral problems were

reported in 36% of patients (5/14), including autism-like behavior (#2, #15), irritability and short attention span (#6, #7, #12). However, no patient had experienced epilepsy.

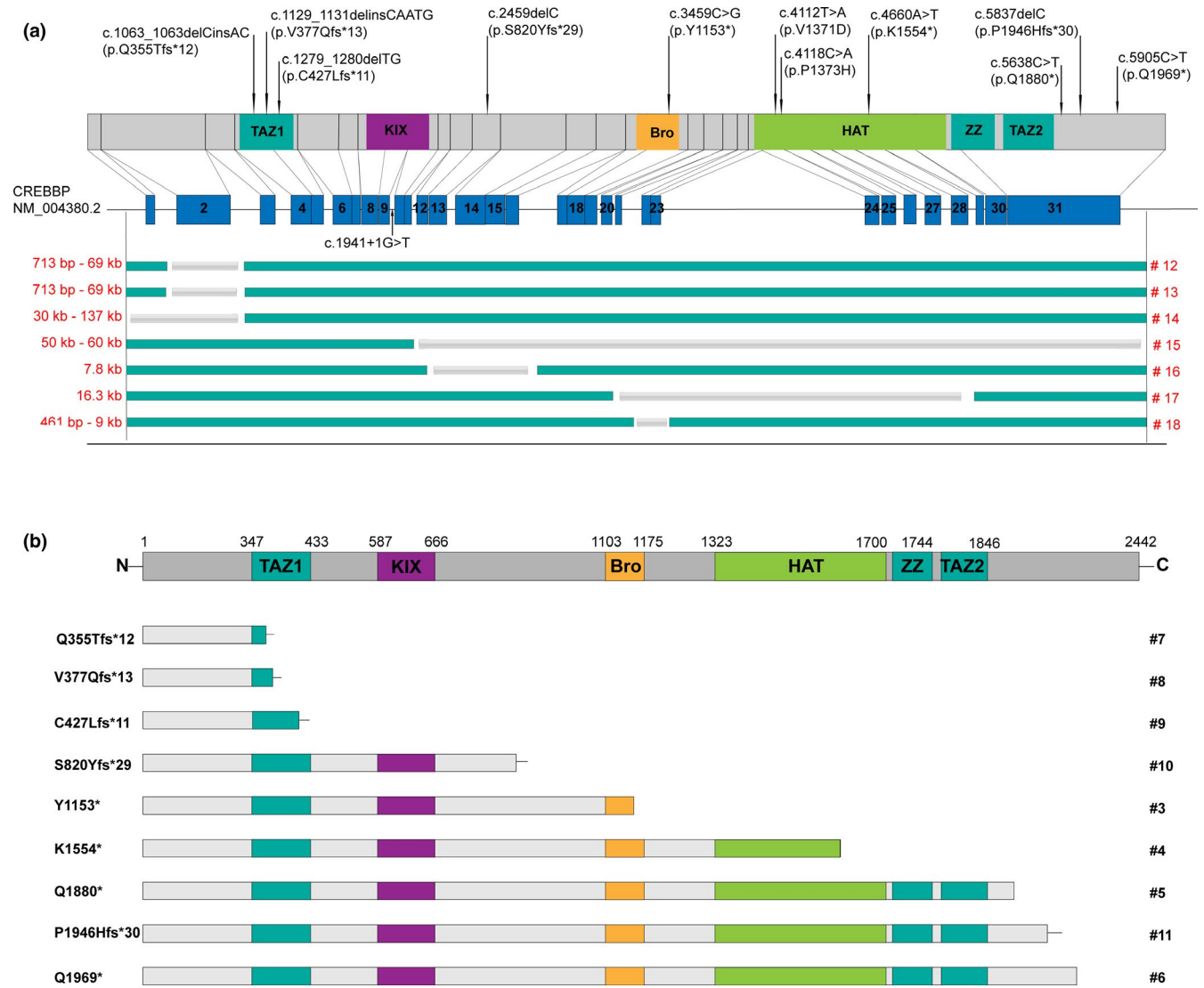


FIGURE 3 Localization on CBP protein of all point mutations and seven deletions (a) and predicted effects of nonsense and frameshift mutations on CBP protein (b). (a) Schematic representation of the CREBBP gene, exons, protein, and its functional domains. The location of variants is depicted by arrows. Seven deletions, depicted by gray bars. TAZ1 = zinc finger, TAZ-type1 (347–433); KIX = CREB-binding domain (587–666); Bro = bromodomain (1,103–1,175); HAT = histone acetyltransferase domain (1,323–1,700); ZZ = zinc finger, ZZ-type (1,701–1,744); TAZ2 = zinc finger, TAZ-type2 (1,765–1,846). Deducted from <http://www.uniprot.org/uniprot/Q92793>. Exons were numbered as in https://www.ncbi.nlm.nih.gov/nucore/NM_004380.2. (b) Schematic representation of wild-type CBP protein and domains. Below, bars indicated the truncated hypothetical CBP proteins, patient number are placed on the right side and the corresponding variants are listed on the left. Solid lines at the C-terminus of the truncated proteins represent aberrant amino acids

3.1.4 | Medical complications

Eleven of 18 (61%) patients were admitted in neonatal intensive care unit (NICU) with severe complications, such as severe pneumonia, hypoglycemia, and septicemia. Five of them (#1, #14, #16, #17, #18) died of severe complications. Seventy percent (12/17) of patients suffered recurrent respiratory tract infections; and 56% (9/16) of patients suffered intractable constipation. However, these symptoms slowly eased with ages, with an average remission age of 21 months for recurrent respiratory tract infections and 28 months of intractable constipation.

Gastroesophageal scintigraphy indicated that patient #4 had pulmonary aspiration (trace), and gastroesophageal reflux was found in patient #6. These two patients were treated with nasogastric tube feeding and got improved.

3.2 | Analysis of the CREBBP gene variants

Nineteen variants of CREBBP gene in 18 patients were identified, including four nonsense, five frameshift, two missense, one splicing variant, and seven intragenic deletions (Table 1, Figure 3). Eighteen heterozygous variants

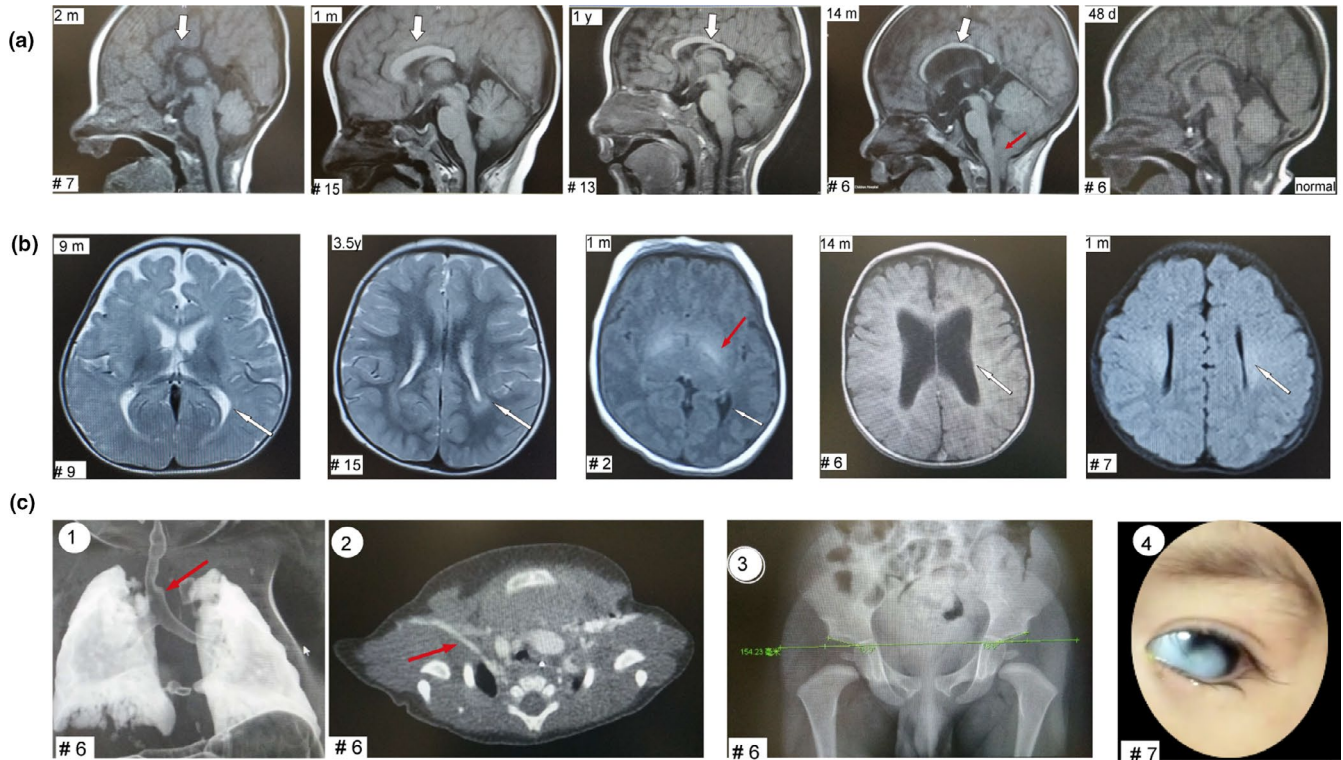


FIGURE 4 Brain MR images (a, b) and other examinations (c) of presently described patients with *CREBBP* mutations. (a) Brain MRI, agenesis of corpus callosum in wide white arrow: #7, complete agenesis; #15, shorter and thickened corpus callosum; #13, shorter corpus callosum; #6, thinner corpus callosum and Chiari type 1 malformation (red arrow) at 14 months. #6 shows normal brain MRI at 48 days. (b) Brain MRI: #9, #15 show delayed myelination (thin white arrow); #2, #6, #7 show abnormality of lateral ventricle (thin white arrow); #2 also shows globus pallidus hyperintensity (red arrow). (c) ① 3D reconstruction of enhanced computed tomography (CT) showing partial esophageal dilatation (red arrow); ② aberrant right subclavian artery (red arrow); ③ squared iliac bones, abnormality of the femora, and small acetabular angle; ④ corneal leucoma. Patient numbers correspond to text, tables, and other figures. d, day; m, month; y, year

are novel, one reported variant (NM_004380.2:c.5837delC, p. Pro1946Hisfs*30) of #11 was found at homozygous state (90%). Besides, all point variants confirmed as de novo, with an exception (NM_004380.2:c.5638C > T, p. Gln1880*), without parental samples, and four of seven deletions were also confirmed as de novo (#12, #15, #16, #18). All variants were classified as pathogenic according to the ACMG criteria. The main clinical findings in different *CREBBP* variant types, including missense, splicing, truncating, and deletions were analyzed, and compared with western populations (Table S2).

Two de novo missense variants NM_004380.2:c.[4112T > A, 4118C > A], p.(Val1371Asp; Pro1373His) were found in cis in patient #2 (Figure 2A). The protein structures affected by the single or double variants were also analyzed. The Val1371 and Pro1373 residues are highly conserved across the different species. Three-dimensional modeling showed that CBP^{V1371D}, CBP^{P1373H}, and CBP^{V1371D + P1373H} did not cause structure changes. However, both of the residues located in the flexure of a loop and the HAT domain of CBP protein. Secondary structure reflected that CBP^{V1371D} causes minor change compared to the CBP^{WT}, CBP^{P1373H}, and CBP^{V1371D + P1373H} proteins.

Four nonsense and five frameshift variations are distributed throughout the *CREBBP* gene, with no hot spot (Figure 3).

However, three truncating variants (NM_004380.2:c.1062dupA, p.Gln355Thrfs*12; NM_004380.2:c.1129_1131delinsCAATG, p.Val377Glnfs*13 and NM_004380.2:c.1279_1280delITG, p.Cys427Leufs*11) were observed clustered in the TAZ1 domain, and another three truncating variants (NM_004380.2:c.5638C > T, p.Gln1880*, NM_004380.2:c.5905C > T, p.Gln1969* and NM_004380.2:c.5837delC, p.Pro1946Hisfs*30) were clustered in exon 31. Six of nine truncating variants are predicted to lead to premature translation stops before or at the HAT domain of CBP. The remaining three variants are predicted to cause the synthesis of a C-terminal-truncated CBP protein which retains all functional domains, including two nonsense variants (#5, #6) and one frameshift variant (#11). For the latter, aberrant amino acid is predicted to synthesis at the C-terminal of the truncated CBP protein. The variant (NM_004380.2:c.5837delC) in the patient #11 was found at homozygous state (90%), with 5/45 raw reads in wild type. Suspicious low heterozygotic peaks can be verified by Sanger sequence. The variant was not detected in her parents' blood DNA (Figure 2B).

The splicing variant (NM_004380.2:c.1941 + 1G>T) at 1-bp splice sites of the codon 647 is predicted to alter the wild-type acceptor site and most probably affect splicing by HSF software (Figure S1).

Seven small heterozygous deletions within *CREBBP* gene were identified by CES and confirmed by qPCR and MLPA. Four deletions (#12, #15, #16, #18) were de novo (Figure S2). Three deletions were observed clustered at the 5' end of the *CREBBP* gene, with #14 involved exon 1–2, and #12, #13 only exon 2. Three deletions (#12, #13, #18) spread in the *CREBBP* gene, and #15 has 20 exons deletion (Table 1, Figure 3).

4 | DISCUSSION AND CONCLUSION

RSTS is a very rare genetic disorder mainly caused by de novo variants in *CREBBP* gene. To date, more than 360 variants in *CREBBP* gene have been described in HGMD (The Human Gene Mutation Database). Deletions of the 16p13.3 have long been recognized as causative in 10% of RSTS patients (Bartsch et al., 1999; Lai et al., 2012).

With the advantages of massively parallel next-generation sequencing (NGS) technologies, clinical and molecular laboratories are now adopting NGS in the genetic testing. In addition, potential disease-causing CNVs can be identified from NGS data except for the SNV findings, and 37% (7/19) of deletions involved *CREBBP* gene from CES were detected. In the reported point variants of *CREBBP* gene, missense variants account for 17%–22% (Lee et al., 2015; Spena, Milani, et al., 2015). However, we found a lower incidence (2%; 2/12) of missense variants of point variants, which reinforces the previous hypothesis that missense variants may account for a very low proportion of RSTS cause (Lee et al., 2015).

Two relative “hot spot” regions in *CREBBP* gene for truncated and deletion variants were observed in our study. One is a 461-nt long region (codons 1931 and 2086) in exon 31 of *CREBBP* gene. Two frameshift and one nonsense clustered in this region (Figure 3). Spena et al. also reported eight of 21 frameshift variations clustered in this region (Spena, Milani, et al., 2015). Hence, this region, especially base pairs 5,837 which have related four frameshift variants involved four RSTS patients (Rokunohe, Nakano, Akasaka, Toyomaki, & Sawamura, 2016; Spena, Milani, et al., 2015), may be a “hot spot” for frameshift and nonsense variants in RSTS patients. Another region locates in exon 2 at the 5' end of the *CREBBP*. Three of seven deletions are embedded in the region in our study. Previous study had demonstrated that repetitive elements (mainly *Alu* and *LINEs*) in this region is significantly higher than that in the entire gene or the average in the genome and pointed out that this region is a peak of breakpoints underlying rearrangements (Gervasini et al., 2007).

Homozygous *Cbp*-deficient mice were revealed embryonic lethality, mental retardation, hemorrhage, neural tube defect, decreased vascularization, and decreased hematopoiesis (Oike et al., 1999; Tanaka et al., 2000). Unexpectedly, a homozygous variant (90%; c.5837delC, p. Pro1946Hisfs*30)

was identified in the blood DNA of patient #11 (Figure 2B). In addition, neither the parents nor the healthy brother, carry this variant in hematologic cells. This frameshift variant has been reported in a 5-year-old Italian girl with RSTS and anomalies of kidney and ureters, with heterozygotes (Spena, Milani, et al., 2015). Different from the reported case, our patient had bilateral cutaneous syndactyly of the second to fourth digits in hands and of 1/2 toes in feet. Her broad angulated thumbs, broad big toes, microcephaly, and facial changes are typical of RSTS (Figure 1). In the follow-up, she was found in delayed developmental milestone but with normal height (Table S1). Other features, such as brain MRI anomalies, urogenital anomalies, and cardiovascular anomalies, were not observed.

Compared with western population, seven clinical features (microcephaly, micrognathia, angulated thumbs, syndactyly, polydactyly, autistic behavior, and epilepsy) are significantly different in our Chinese patients ($p < .05$; Table S2). None of these 18 patients displayed epilepsy which is frequent in RSTS patients with *CREBBP* variants; more patients had microcephaly and micrognathia; few patients had angulated thumbs. Herein, ethnic heterogeneity may contribute to the differences. However, the average age of our patients is 32 months currently, in whom epilepsy may not yet have appeared. Simultaneously, the reason of population special cannot be excluded.

Polydactyly and syndactyly have been rarely reported in RSTS patients (Milani et al., 2015). However, a high incidence (7/19, 37%) of polydactyly and/or syndactyly was observed in our study. Postaxial polydactyly is more common (80%) than preaxial polydactyly (20%), different from the previous study which showed preaxial polydactyly (3/4) is more common (Spena, Milani, et al., 2015). The syndactyly exhibits great clinical variability. Two patients had bilateral cutaneous syndactyly of the second to fourth digits of the hands, although they had different syndactyly of toes (#6 had bilateral syndactyly of 1/2 and 3/4 toes, #11 had bilateral syndactyly of 1/2 toes). Patient #4 had unusual bilateral bifid big toe and patient #1 had unilateral bifid small toe. Therefore, the polydactyly and/or syndactyly of hands and feet may be a hallmark of RSTS and more prevalent in patients with point variants.

Our study found that corpus callosum anomalies (agenesis or dysmorphisms) are the most frequent MRI anomalies in RSTS patients, 29% of patients had corpus callosum anomalies ranged from mild to severe (Figure 4). Delayed myelination was observed in 21% of patients. It should be noted that in patient #6, brain MRI at 48 days was reported as normal; however, at 14 months, the MRI showed Chiari malformation type I, corpus callosum thinner, and hydrocephaly. Chiari malformations have been described frequently in RSTS in association with craniovertebral junction anomalies (Ajmone et al., 2018).

Recurrent upper respiratory infections and severe constipation are common complications in RSTS patients (Milani et al., 2015), while the pathogenesis is still unknown. Seventy percent (12/17) of patients suffered recurrent respiratory tract

infections; and 56% (9/16) of patients had intractable constipation. Gastroesophageal reflux and pulmonary aspiration (trace) may be possible causes for recurrent upper respiratory infection in patients #4 and #6. However, these symptoms were observed slowly eased with ages, with an average remission age of 21 months for recurrent respiratory tract infections and 28 months for intractable constipation. This finding may provide professional management and follow-up care to RSTS.

Obesity can be onset in adolescence in RSTS patients (Milani et al., 2015). To our knowledge, only a 9-year-old boy RSTS patients was reported obesity in childhood (Zuconi, Ferini-Strambi, Erminio, Pestalozza, & Smirne, 1993). However, a Uyghur origin girl presented with obesity and hyperphagia from 7 months in our study. Her weight was $>>3 SD$, BMI was 35 at age 12 and with short stature ($< -2 SD$). She has been studying in normal school, but could not write words or calculate, with mild developmental delay. She was suspected with Prader–Willi syndrome at the age of 10; however, her Prader–Willi syndrome DNA methylation testing revealed a negative result.

In conclusion, we analyzed 18 RSTS patients with 19 novel variants in *CREBBP* gene in Chinese population. Our results reveal critical insights into the genetic and phenotypic heterogeneity of RSTS and show key differences in the phenotypes among different populations. Furthermore, our study illustrates the value of applying CES to optimize the detection of *CREBBP* variants/deletions.

ACKNOWLEDGMENTS

We are grateful to the clinicians who take care of the patients, patients and their parents who trust our laboratory. We are also grateful to the colleagues of our genetic laboratory teams for providing technical testing. This work was supported by the fund of National Natural Science Foundation of China (81741036), the National Key Research and Development Program (2018YFC0116903) and Shanghai Key Laboratory of Birth Defects (13DZ2260600).

CONFLICT OF INTEREST

The authors declare no conflict of interest.

DATA AVAILABILITY STATEMENT

The data that support the findings of this study are available on request from the corresponding author. The data are not publicly available due to privacy or ethical restrictions.

ORCID

Sha Yu  <https://orcid.org/0000-0002-8487-974X>

Ping Zhang  <https://orcid.org/0000-0003-2343-4189>

Huijun Wang  <https://orcid.org/0000-0002-9992-6457>

REFERENCES

- Adzhubei, I. A., Schmidt, S., Peshkin, L., Ramensky, V. E., Gerasimova, A., Bork, P., ... Sunyaev, S. R. (2010). A method and server for predicting damaging missense mutations. *Nature Methods*, 7(4), 248–249. <https://doi.org/10.1038/nmeth0410-248>
- Ajmone, P. F., Avignone, S., Gervasini, C., Giacobbe, A., Monti, F., Costantino, A., ... Milani, D. (2018). Rubinstein-Taybi syndrome: New neuroradiological and neuropsychiatric insights from a multidisciplinary approach. *American Journal of Medical Genetics Part B: Neuropsychiatric Genetics*, 177(4), 406–415. <https://doi.org/10.1002/ajmg.b.32628>
- Backenroth, D., Homsy, J., Murillo, L. R., Glessner, J., Lin, E., Brueckner, M., ... Shen, Y. (2014). CANOES: Detecting rare copy number variants from whole exome sequencing data. *Nucleic Acids Research*, 42(12), e97. <https://doi.org/10.1093/nar/gku345>
- Bartsch, O., Kress, W., Kempf, O., Lechno, S., Haaf, T., & Zechner, U. (2010). Inheritance and variable expression in Rubinstein-Taybi syndrome. *American Journal of Medical Genetics. Part A*, 152A(9), 2254–2261. <https://doi.org/10.1002/ajmg.a.33598>
- Bartsch, O., Wagner, A., Hinkel, G. K., Krebs, P., Stumm, M., Schmalenberger, B., ... Majewski, F. (1999). FISH studies in 45 patients with Rubinstein-Taybi syndrome: Deletions associated with polysplenia, hypoplastic left heart and death in infancy. *European Journal of Human Genetics*, 7(7), 748–756. <https://doi.org/10.1038/sj.ejhg.5200378>
- Chan, H. M., & Thangue, N. B. L. (2001). p300/CBP proteins: HATs for transcriptional bridges and scaffolds. *Journal of Cell Science*, 114(13), 2363–2373. Retrieved from <http://jcs.biologists.org/content/114/13/2363>
- Desmet, F.-O., Hamroun, D., Lalande, M., Collod-Bérout, G., Claustres, M., & Bérout, C. (2009). Human Splicing Finder: An online bioinformatics tool to predict splicing signals. *Nucleic Acids Research*, 37(9), e67. <https://doi.org/10.1093/nar/gkp215>
- Ellingford, J. M., Campbell, C., Barton, S., Bhaskar, S., Gupta, S., Taylor, R. L., ... Black, G. C. M. (2017). Validation of copy number variation analysis for next-generation sequencing diagnostics. *European Journal of Human Genetics*, 25(6), 719–724. <https://doi.org/10.1038/ejhg.2017.42>
- Gervasini, C., Castronovo, P., Bentivegna, A., Mottadelli, F., Faravelli, F., Giovannucci-Uzielli, M. L., ... Larizza, L. (2007). High frequency of mosaic *CREBBP* deletions in Rubinstein-Taybi syndrome patients and mapping of somatic and germ-line breakpoints. *Genomics*, 90(5), 567–573. <https://doi.org/10.1016/j.ygeno.2007.07.012>
- Hennekam, R. C. M. (2006). Rubinstein-Taybi syndrome. *European Journal of Human Genetics*, 14(9), 981–985. <https://doi.org/10.1038/sj.ejhg.5201594>
- Kalkhoven, E., Roelfsema, J. H., Teunissen, H., den Boer, A., Ariyurek, Y., Zantema, A., ... Peters, D. J. M. (2003). Loss of CBP acetyltransferase activity by PHD finger mutations in Rubinstein-Taybi syndrome. *Human Molecular Genetics*, 12(4), 441–450. <https://doi.org/10.1093/hmg/ddg039>
- Lai, A. H. M., Brett, M. S., Chin, W.-H., Lim, E. C. P., Ng, J. S. H., & Tan, E.-C. (2012). A submicroscopic deletion involving part of the *CREBBP* gene detected by array-CGH in a patient with Rubinstein-Taybi syndrome. *Gene*, 499(1), 182–185. <https://doi.org/10.1016/j.gene.2012.02.043>
- Lee, H., Deignan, J. L., Dorrani, N., Strom, S. P., Kantarci, S., Quintero-Rivera, F., ... Nelson, S. F. (2014). Clinical exome sequencing for

- genetic identification of rare Mendelian disorders. *JAMA*, 312(18), 1880. <https://doi.org/10.1001/jama.2014.14604>
- Lee, J. S., Byun, C. K., Kim, H., Lim, B. C., Hwang, H., Choi, J. E., ... Chae, J.-H. (2015). Clinical and mutational spectrum in Korean patients with Rubinstein-Taybi syndrome: The spectrum of brain MRI abnormalities. *Brain and Development*, 37(4), 402–408. <https://doi.org/10.1016/j.braindev.2014.07.007>
- Li, H. (2009). [Growth standardized values and curves based on weight, length/height and head circumference for Chinese children under 7 years of age]. *Zhonghua Er Ke Za Zhi = Chinese Journal of Pediatrics*, 47(3), 173–178.
- Martí-Renom, M. A., Stuart, A. C., Fiser, A., Sánchez, R., Melo, F., & Šali, A. (2000). Comparative protein structure modeling of genes and genomes. *Annual Review of Biophysics and Biomolecular Structure*, 29(1), 291–325. <https://doi.org/10.1146/annurev.biophys.29.1.291>
- McLaren, W., Pritchard, B., Rios, D., Chen, Y., Flicek, P., & Cunningham, F. (2010). Deriving the consequences of genomic variants with the Ensembl API and SNP Effect Predictor. *Bioinformatics*, 26(16), 2069–2070. <https://doi.org/10.1093/bioinformatics/btq330>
- Milani, D., Manzoni, F. M. P., Pezzani, L., Ajmone, P., Gervasini, C., Menni, F., & Esposito, S. (2015). Rubinstein-Taybi syndrome: Clinical features, genetic basis, diagnosis, and management. *Italian Journal of Pediatrics*, 41, 4. <https://doi.org/10.1186/s13052-015-0110-1>
- Negri, G., Milani, D., Colapietro, P., Forzano, F., Della Monica, M., Rusconi, D., ... Gervasini, C. (2015). Clinical and molecular characterization of Rubinstein-Taybi syndrome patients carrying distinct novel mutations of the EP300 gene. *Clinical Genetics*, 87(2), 148–154. <https://doi.org/10.1111/cge.12348>
- Oike, Y., Hata, A., Mamiya, T., Kaname, T., Noda, Y., Suzuki, M., ... Yamamura, K. (1999). Truncated CBP protein leads to classical Rubinstein-Taybi syndrome phenotypes in mice: Implications for a dominant-negative mechanism. *Human Molecular Genetics*, 8(3), 387–396. <https://doi.org/10.1093/hmg/8.3.387>
- Park, S., Stanfield, R. L., Martinez-Yamout, M. A., Dyson, H. J., Wilson, I. A., & Wright, P. E. (2017). Role of the CBP catalytic core in intramolecular SUMOylation and control of histone H3 acetylation. *Proceedings of the National Academy of Sciences of the United States of America*, 114(27), E5335–E5342. <https://doi.org/10.1073/pnas.1703105114>
- Kumar, P., Henikoff, S., & Ng, P. C. (2009). Predicting the effects of coding non-synonymous variants on protein function using the SIFT algorithm. *Nature Protocols*, 4(7), 1073–1081. <https://doi.org/10.1038/nprot.2009.86>
- Qian, Q. B. L., Lin, Y., Bing-bing, W., Hui-jun, W., Xin-ran, D., Yu-lan, L., & Wen-hao, Z. (2018). Application of copy number variation screening analysis process based on high-throughput sequencing technology. *Chinese Journal of Evidence-Based Pediatric*, 13, 275–279.
- Richards, S., Aziz, N., Bale, S., Bick, D., Das, S., Gastier-Foster, J., ... Rehm, H. L. (2015). Standards and guidelines for the interpretation of sequence variants: A joint consensus recommendation of the American College of Medical Genetics and Genomics and the Association for Molecular Pathology. *Genetics in Medicine*, 17(5), 405–424. <https://doi.org/10.1038/gim.2015.30>
- Rokunohe, D., Nakano, H., Akasaka, E., Toyomaki, Y., & Sawamura, D. (2016). Rubinstein-Taybi syndrome with multiple pilomatricomas: The first case diagnosed by CREBBP mutation analysis. *Journal of Dermatological Science*, 83(3), 240–242. <https://doi.org/10.1016/j.jdermsci.2016.06.005>
- Rubinstein, J. H., & Taybi, H. (1963). Broad thumbs and toes and facial abnormalities. A possible mental retardation syndrome. *American Journal of Diseases of Children*, 105(6), 588–608. <https://doi.org/10.1001/archpedi.1963.02080040590010>
- Rusconi, D., Negri, G., Colapietro, P., Picinelli, C., Milani, D., Spena, S., ... Gervasini, C. (2015). Characterization of 14 novel deletions underlying Rubinstein-Taybi syndrome: An update of the CREBBP deletion repertoire. *Human Genetics*, 134(6), 613–626. <https://doi.org/10.1007/s00439-015-1542-9>
- Schmittgen, T. D., & Livak, K. J. (2008). Analyzing real-time PCR data by the comparative C(T) method. *Nature Protocols*, 3(6), 1101–1108. <https://doi.org/10.1038/nprot.2008.73>
- Schouten, J. P. (2002). Relative quantification of 40 nucleic acid sequences by multiplex ligation-dependent probe amplification. *Nucleic Acids Research*, 30(12), 57e–557. <https://doi.org/10.1093/nar/gnf056>
- Schwarz, J. M., Rödelberger, C., Schuelke, M., & Seelow, D. (2010). MutationTaster evaluates disease-causing potential of sequence alterations. *Nature Methods*, 7(8), 575–576. <https://doi.org/10.1038/nmeth0810-575>
- Shiama, N. (1997). The p300/CBP family: Integrating signals with transcription factors and chromatin. *Trends in Cell Biology*, 7(6), 230–236. [https://doi.org/10.1016/S0962-8924\(97\)01048-9](https://doi.org/10.1016/S0962-8924(97)01048-9)
- Spena, S., Gervasini, C., & Milani, D. (2015). Ultra-rare syndromes: The example of Rubinstein-Taybi syndrome. *Journal of Pediatric Genetics*, 4(3), 177–186. <https://doi.org/10.1055/s-0035-1564571>
- Spena, S., Milani, D., Rusconi, D., Negri, G., Colapietro, P., Elcioglu, N., ... Gervasini, C. (2015). Insights into genotype-phenotype correlations from CREBBP point mutation screening in a cohort of 46 Rubinstein-Taybi syndrome patients. *Clinical Genetics*, 88(5), 431–440. <https://doi.org/10.1111/cge.12537>
- Tanaka, Y., Naruse, I., Hongo, T., Xu, M., Nakahata, T., Maekawa, T., & Ishii, S. (2000). Extensive brain hemorrhage and embryonic lethality in a mouse null mutant of CREB-binding protein. *Mechanisms of Development*, 95(1–2), 133–145. [https://doi.org/10.1016/S0925-4773\(00\)00360-9](https://doi.org/10.1016/S0925-4773(00)00360-9)
- Zhu, L., Zhang, R., Zhang, S., Shi, W., Yan, W., Wang, X., ... Chinese Neonatal Network. (2015). [Chinese neonatal birth weight curve for different gestational age]. *Zhonghua Er Ke Za Zhi = Chinese Journal of Pediatrics*, 53(2), 97–103.
- Zucconi, M., Ferini-Strambi, L., Erminio, C., Pestalozza, G., & Smirne, S. (1993). Obstructive sleep apnea in the Rubinstein-Taybi syndrome. *Respiration; International Review of Thoracic Diseases*, 60(2), 127–132. <https://doi.org/10.1159/000196186>

SUPPORTING INFORMATION

Additional supporting information may be found online in the Supporting Information section.

How to cite this article: Yu S, Wu B, Qian Y, et al. Clinical exome sequencing identifies novel *CREBBP* variants in 18 Chinese Rubinstein-Taybi Syndrome kids with high frequency of polydactyly. *Mol Genet Genomic Med*. 2019;7:e1009. <https://doi.org/10.1002/mgg3.1009>